2006-1008: FOUR HARDWARE EXPERIMENTS FOR ADVANCED DYNAMICS AND CONTROL

Bradley Burchett, Rose-Hulman Institute of Technology

BRADLEY T BURCHETT is an Assistant Professor of Mechanical Engineering. He teaches courses on the topics of dynamics, system dynamics, control, intelligent control, and computer applications. His research interests include non-linear and intelligent control of autonomous vehicles, and numerical methods applied to optimal control.

Four Hardware Experiments for Advanced Dynamics and Control

Bradley T. Burchett

Department of Mechanical Engineering, Rose-Hulman Institute of Technology, Terre Haute, IN 47803

Abstract

The faculty of the mechanical and electrical engineering departments at Rose-Hulman Institute of Technology have developed many experiments for system modeling and control. In this work, we present the development of additional experiments intended to broaden the repertoire of courses in which the controls lab hardware is used. First, we capitalize on previous modeling experiments using both step response and frequency response to precisely identify the parameters of linear and radial hanging crane models. Second, students use the stable model obtained through frequency response to form the open-loop unstable model of the plant in inverted pendulum mode. They then apply Ackermann's formula to obtain the state feedback gains to place the closed loop poles at locations suggested by the professor. Third, we present a state feedback control experiment based on a two degree of freedom mass-spring system with rigid body mode. Control of this device is analogous to control through a flexible manipulator, except that the system is simplified to one-dimensional motion. Fourth, we show a proposed modeling and parameter identification laboratory for a graduate level dynamics course. Students are required to develop the system non-linear kinematic equations, then apply LaGrange's formulae to obtain two degree of freedom kinetic equations. They are then expected to obtain experimental response data, and provide precise estimates of system physical parameters through matching theoretical response with experimental.

Introduction

We have developed a series of four advanced modeling and control labs for use in the senior level introductory controls course and the graduate level advanced dynamics course. The ECP Model 210 Rectilinear Control System (ECP210) and the ECP Model 205 Torsional Control System (ECP205)[1] are used for these experiments. These commercially available plants are precisely instrumented mechanical systems that are user configurable for a wide variety of degrees of freedom and plant parameters. Although very different in appearance, the components of stiffness, inertia and damping are completely analogous between the systems, and using both in the lab provides an opportunity to emphasize the concept of system analogy. That is, the form of the state space models is identical, only the parameters and units change when moving from rectilinear to torsional and back. The ECP210 and ECP205 are shown in Figures 1a and 1b respectively.

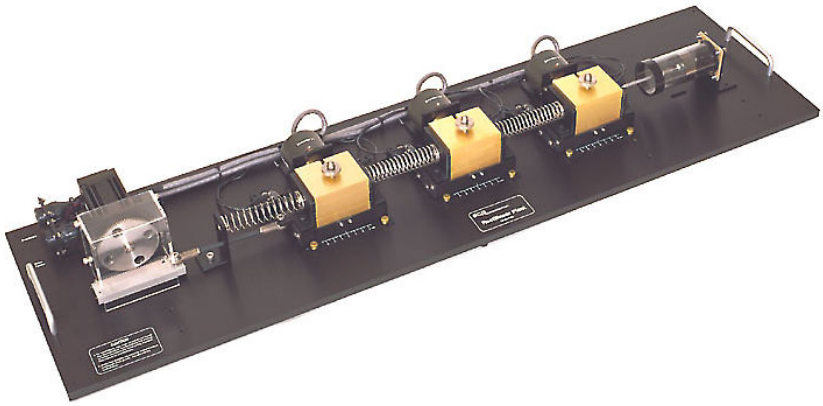

Fig. 1a. The ECP Rectilinear Control System (ECP 210)

Fig. 1b. The ECP 205

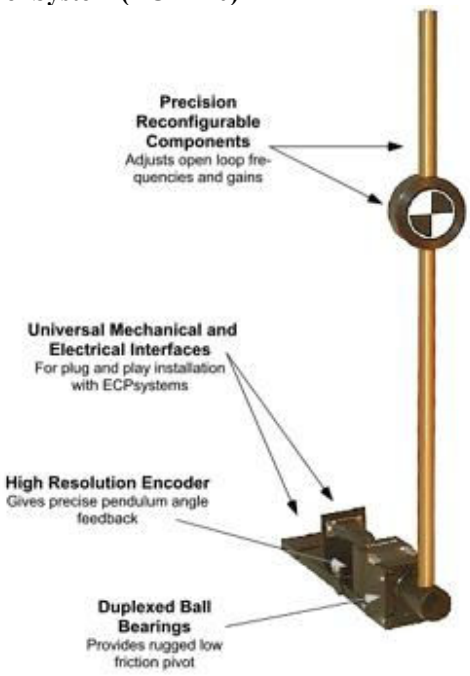

Fig 1c. Inverted Pendulum Accessory

In addition, the first and second and fourth experiments described below use the Inverted Pendulum Accessory (ECP A51). The ECP A51 consists of a base attachment with an instrumented revolute joint for attaching the pendulum, and the pendulum itself which is a hollow brass rod with a moveable additional disk shaped mass. This is an add-on feature that provides the capability of performing the historically renowned stick balancing problem using either the first cart of ECP210 or the first disk of ECP205 as the base.

Section 2 describes the cart (disk) / pendulum parameter identification procedure. Section 3 outlines inverted pendulum and Furuta[2] pendulum experiments. Section 4 discusses control through a flexible manipulator experiment. Section 5 presents the advanced dynamics spatial, non-linear free-response experiment. Section 6 shows assessment data from the senior level controls class which performed the first three experiments.

Experimental Parameter Identification of Inverted Pendulum and Furuta Pendulum

The Furuta Pendulum[2] (FP) systems are represented in the crane or hanging mode by the schematics shown in Figure 3. Figure 3 shows the symbols and sign conventions that will be used in describing experiments 1, 2 and 4. The Inverted Pendulum (IP) and FP are famous control experiments since they require feedback stabilization of an open-loop unstable plant. Thus the significant modeling challenge is how to experimentally determine the physical parameters without knowing *a priori* a stabilizing control law. This challenge is answered by observing that the system has both stable (hanging or crane mode) and unstable (inverted) equilibria. The physical parameters are not changed by changing mode, and we shall see shortly that the state space models differ only by sign on a few terms. The same can be said of the IP, and the corresponding equations are shown in the Appendix.

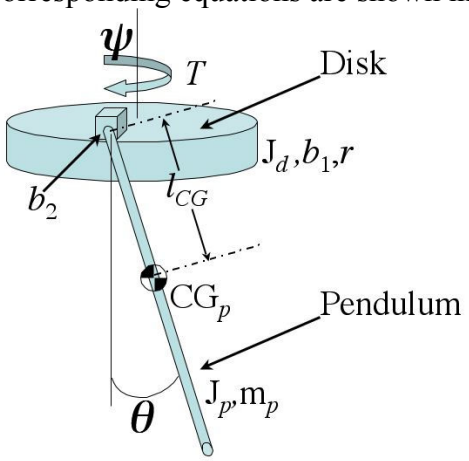

Fig. 3a. Schematic of the Furuta Pendulum in Crane Mode

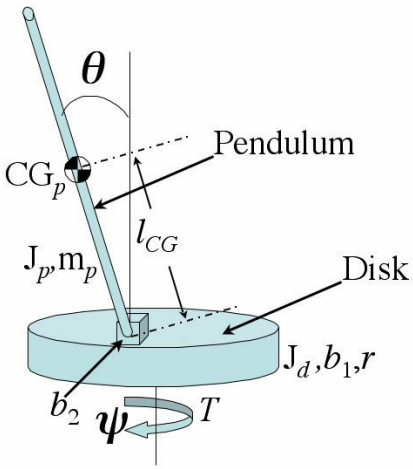

Fig. 3b. Schematic of the Furuta Pendulum in Inverted Mode

First principle modeling, followed by Taylor series linearization results in the following state-space model for the Furuta pendulum in crane mode:

$$\dot{\mathbf{x}} = \mathbf{A}\mathbf{x} + \mathbf{B}T \qquad \mathbf{y} = \mathbf{C}\mathbf{x} \tag{1}$$

Where, $\mathbf{x}$ is the state vector consisting of base disk twist angle ψ and angular velocity $\dot{\psi}$, and pendulum swing angle θ angular velocity $\dot{\theta}$.

$$\mathbf{x} = \begin{bmatrix} \psi & \dot{\psi} & \theta & \dot{\theta} \end{bmatrix}^T$$

As illustrated above, r is the distance from the center axis of the base disk to pendulum longitudinal axis, J_d and J_p are the disk and pendulum centroidal moments of inertia respectively, b_1 and b_2 are revolute joint viscous damping, T is the applied control torque, l_{CG} is the distance from mounting joint to pendulum center of gravity, and m_p is the pendulum mass.

The state space parameter matrices are

$$\mathbf{A} = \begin{bmatrix} 0 & 1 & 0 & 0 \\ 0 & \dfrac{-J_A b_1}{D_2} & -\dfrac{m_p^2 l_{cg}^2 r g}{D_2} & -\dfrac{m_p l_{cg} r b_2}{D_2} \\ 0 & 0 & 0 & 1 \\ 0 & -\dfrac{m_p l_{cg} b_1}{D_2} & -\dfrac{\left(m_p r^2 + J_d\right) m_p l_{cg} g}{D_2} & -\dfrac{\left(m_p r^2 + J_d\right) b_2}{D_2} \end{bmatrix},$$

$$\mathbf{B} = \begin{bmatrix} 0 & \dfrac{J_A}{D_2} & 0 & \dfrac{m_p l_{cg} r}{D_2} \end{bmatrix}^{\mathrm{T}}$$

and

$$\mathbf{C} = \begin{bmatrix} K_1 & 0 & 0 & 0 \\ 0 & 0 & K_2 & 0 \end{bmatrix}.$$

Where K_1 and K_2 are static gains, D_2 is a combination term

$$D_2 = J_A\left(J_d + m_p r^2\right) + m_p^2 l_{cg}^2 r^2$$

and J_A is the pendulum moment of inertia about its mounting joint.

$$J_A = J_p + m_p l_{cg}^2.$$

The corresponding transfer functions are

$$\frac{\psi(s)}{T(s)} = K_1 \frac{J_A D_2 s^2 + \left(J_A b_2\left(m_p r^2 + J_d\right) - m_p^2 l_{cg}^2 b_2 r^2\right)s + J_A m_p g l_{cg}\left(m_p r^2 + J_d\right) - m_p^3 l_{cg}^3 g r^2}{s\Delta_2}$$

and

$$\frac{\theta(s)}{T(s)} = -K_2 \frac{m_p l_{cg} r D_2 s}{\Delta_2}$$

Where Δ_2 is the system determinant

$$\begin{aligned} \Delta_2 = {} & D^2 s^3 + \left(D_2 b_2 m_p r^2 + D_2\left(J_A b_1 + J_d b_2\right)\right)s^2 \\ & + \left(D_2 m_p g l_{cg}\left(m_p r^2 + J_d\right) + J_A b_1 b_2\left(m_p r^2 + J_d\right) - m_p^2 l_{cg}^2 r^2 b_1 b_2\right)s \\ & + J_A b_1 m_p g l_{cg}\left(m_p r^2 + J_d\right) - m_p^3 l_{cg}^3 r^2 b_1 g \end{aligned}.$$

In order to precisely determine the physical parameters of the Inverted Pendulum (IP) and Furuta Pendulum (FP) systems, each system is first subdivided into a one degree-of-freedom (DOF) model consisting of the base cart (disk) with a stiffness and damper attached. For the linear case, the one DOF system can be modeled according to the schematic shown in Figure 4 below.

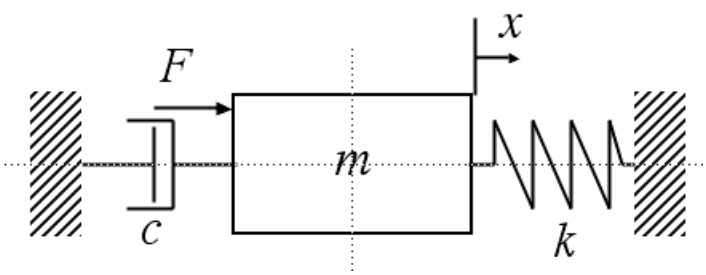

Fig. 4. Schematic of One DOF System

The inertia of the linear cart can be systematically varied by adding 500g masses underneath the ECP X base attachment. In the torsional case, 500g masses can be added, and moved between 2 and 9cm from the disk center. The effective change in moment of inertia is thus known through a simple calculation involving the parallel axis theorem. By taking step responses with at least three different inertia configurations, the students use a technique from reference 3 to determine the stiffness value and inertia of cart (disk) with base attachment. The students used this technique in the course's first lab, so they are quite familiar with it.

After finding the inertia parameter of the one DOF system, the students assemble the overall system and take experimental frequency response data. A simplex-based search is used to minimize the squared difference (in dB) between experimental and theoretical frequency response data. For complete details of this method, see reference 4. This method is rather sensitive to initial guesses, therefore, the data is first fitted to the transfer function from input force to pendulum swing angle to refine initial guesses of the system parameters, before fitting to the full two DOF state space model.

A typical result of fitting experimental frequency response data from the Furuta Pendulum is shown in Figure 5 below.

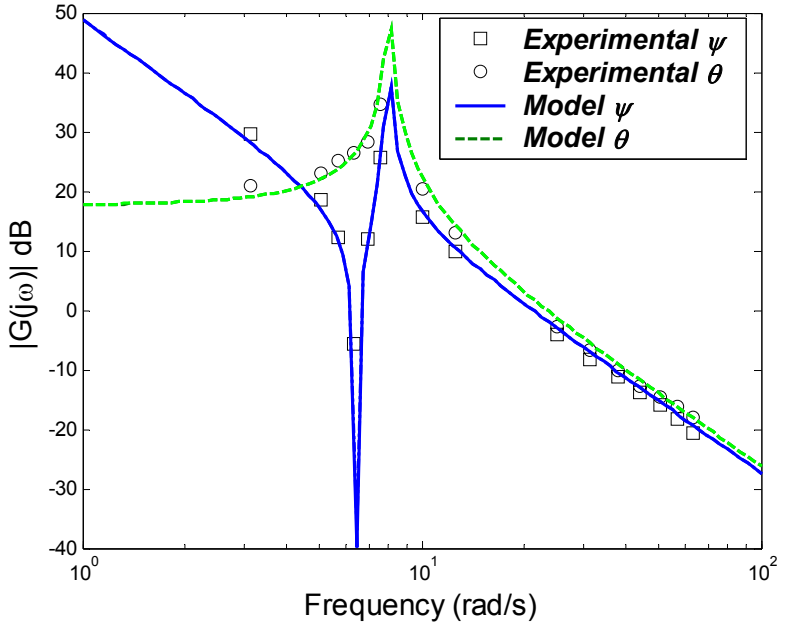

Figure 5: Sample result from fitting frequency response data to ECP 205 model with pendulum accessory

State Feedback Regulation of the Inverted Pendulum and Furuta Pendulum

Applying first principles to the Furuta Pendulum near the inverted equilibrium point, and performing a Taylor Series linearization, we obtain the following state space model.

$$\dot{\mathbf{x}} = \mathbf{A}\mathbf{x} + \mathbf{B}T \qquad \mathbf{y} = \mathbf{C}\mathbf{x} \tag{2}$$

Where all symbols retain their previous definitions. The state space matrices are

$$\mathbf{A} = \begin{bmatrix} 0 & 1 & 0 & 0 \\ 0 & \dfrac{-J_A b_1}{D_2} & -\dfrac{m_p^2 l_{cg}^2 r g}{D_2} & \dfrac{m_p l_{cg} r b_2}{D_2} \\ 0 & 0 & 0 & 1 \\ 0 & \dfrac{m_p l_{cg} b_1}{D_2} & \dfrac{\left(m_p r^2 + J_d\right) m_p l_{cg} g}{D_2} & -\dfrac{\left(m_p r^2 + J_d\right) b_2}{D_2} \end{bmatrix},$$

$$\mathbf{B} = \begin{bmatrix} 0 & \dfrac{J_A}{D_2} & 0 & -\dfrac{m_p l_{cg} r}{D_2} \end{bmatrix}^{\mathrm{T}},$$

and

$$\mathbf{C} = \begin{bmatrix} K_1 & 0 & 0 & 0 \\ 0 & 0 & K_2 & 0 \end{bmatrix}$$

$$\mathbf{x} = \begin{bmatrix} \psi & \dot{\psi} & \theta & \dot{\theta} \end{bmatrix}^T$$

$$D_2 = J_A\left(J_d + m_p r^2\right) + m_p^2 l_{cg}^2 r^2$$

and

$$J_A = J_p + m_p l_{cg}^2.$$

Clearly the **A** matrix in Eqn. 2 differs from the **A** matrix in Eqn. 1 merely by a few sign changes. Thus, knowing the physical parameters of the IP and FP in crane mode, the students can easily formulate a state space model of the IP and/or FP in inverted mode. The equations for the linear IP are shown in the Appendix.

In this experiment, the students determine an appropriate set of state feedback gains for the IP or FP by applying Ackermann's formula to the model given above. Closed-loop pole locations are suggested by the professor based on an LQR design from a nominal plant model. The professor determined several sets of LQR gains close to the actuator saturation limits. The suggested pole locations for the FP are shown in Table 1 below.

Table 1. Suggested Closed-loop pole locations for State Feedback Regulator Design, FP

Set 1	Set 2	Set 3	Set 4
s = -4.1484 ±1.6341j	s = -4.4305 ± 2.0497 j	s = -4.5628 ± 2.2419 j	s = -4.6314 ± 2.3357 j
-16.8545	-21.915	-29.5357	-40.7029
-3.2220	-2.9234	-2.8285	-2.7882

The Simulink real-time interface is configured to give the control architecture shown in Figure 6. Here x_1 is the base disk twist angle, and x_2 is the pendulum swing angle. The hardware encoders provide position measurements only, thus the velocity states are determined by numerical differentiation. Since this is a regulation problem, i.e., the set point is zero, the prefilter gain k_{pf} is set to zero. Calculation of the pre-filter gain or 'outer loop design' is reserved for the third experiment.

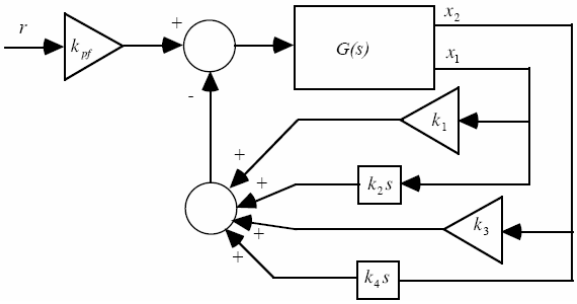

Fig. 6. State Feedback Control Architecture

Typically at least two of the pole locations result in successful closed-loop regulation of the IP or FP system, and at least one results in either actuator saturation or insufficient control effort. In a few cases, the sensors were discovered to be improperly scaled. All of these experiences are valuable in reinforcing the importance of actuator limitations, and accurate sensing in feedback systems. We will expound on these observations in the sequel.

State Feedback Tracking Control of a Flexible Manipulator

The ECP 210 or ECP 205 is used in this experiment. The system is configured in two DOF mode with one rigid and one flexible mode as shown in Figure 7. An analogous torsional schematic may be drawn of the ECP 205 by simply changing the coordinates and parameters to their angular equivalents.

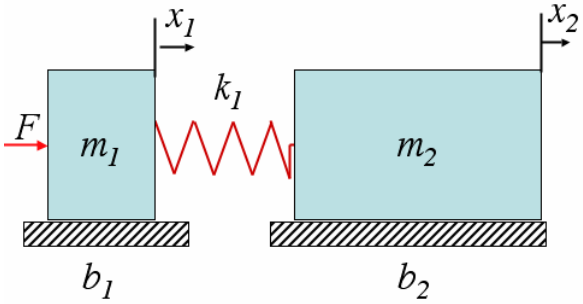

Fig. 7. Schematic of two DOF flexible system.

The students have determined accurate values of the physical parameters of the two DOF flexible system through experiments described in References 2 and 3. Students use Ackermann's formula to directly place the closed-loop poles at desired locations using state feedback. In addition to finding the state feedback gains shown in Figure 6, they must also

compute the prefilter gain k_{pf}. The professor provides four sets of good closed-loop poles based on the LQR root locus. The four pole sets are shown in Table 2, and were chosen by progressively decreasing the control effort penalty in the LQR solution. Pole set four pushes the system performance near the actuator saturation limit on most systems. Since the feedback gains are unique for any specified set of closed-loop poles, the feedback gains found using Ackermann's formula will be identical to the LQR gains. Performance is shown to improve drastically by using state feedback. Since the plant model varies significantly between set-ups, the actual LQR pole locations will also vary, however, the controller found using LQR is very robust, and thus the student designed state feedback controller is also very robust.

Table 2. Suggested Closed-loop pole locations for State Feedback Tracker Design, ECP 210

Set 1	Set 2	Set 3	Set 4
s = -7.533 ±27.28j	s = -8.7164 ±26.7j	s = -9.3632 ±26.0j	s = -9.6046 ±25.516j
-18.53 ±10.35j	-23.59 ±9.53j	-35.1	-60.124
		-26.96	-22.841

Free Response Modeling and Parameter Estimation of Rotary Pendulum with Large Deflections

A major challenge in teaching three-dimensional rigid body dynamics is that of finding well-instrumented mechanical systems for realistic experiments. The ECP205 with ECP X attachment provides an excellent example. A schematic of the system is provided in Figure 3a. The system provides two rotations (shown as ψ and θ in Figure 3a) along axes that are mutually orthogonal in space. Each of these rotations is precisely measured using optical encoders.

Given two arbitrary rotations about mutually orthogonal axes, kinematic law states that the body (pendulum in this case) can be positioned in an arbitrary rotation in space. Thus, this system is 'truly spatial'. Determining the dynamic model of this system requires full three-dimensional kinematics. Even without precise instrumentation, the physical system provides an excellent opportunity to illustrate the finite rotation relationship between three frames which are required to describe the kinematics. For example, the professor chose a fixed reference frame with one axis pointed vertically down, making the ψ rotation positive about one of the fixed reference frame axes. The intermediate frame is related to the fixed frame by the ψ rotation. The second axis of the intermediate frame is chosen to point directly outward through the revolute joint. Thus, the body frame is related to the intermediate frame through a simple rotation corresponding to rotation about the revolute joint.

Because of the system complexity, students are encouraged to use Lagrange's equations to find the differential equations of motion. The result is shown as Eqn. 3.

$$\mathbf{A}\begin{Bmatrix}\ddot{\psi}\\ \ddot{\theta}\end{Bmatrix} = \mathbf{b}\left(\psi,\theta,\dot{\psi},\dot{\theta}\right) \tag{3}$$

Where

$$\mathbf{A} = \begin{bmatrix} m_p r^2 + \left(m_p l_{cg}^2 + J_{zz}\right)s_\theta^2 + J_{xx}c_\theta^2 + J_d & -m_p r l_{cg} c_\theta \\ -m_p r l_{cg} c_\theta & m_p l_{cg}^2 + J_{zz} \end{bmatrix}$$

And

$$\mathbf{b} = \begin{Bmatrix} -2\dot{\theta}\dot{\psi}s_\theta c_\theta\left(m_p l_{cg}^2 + J_{zz} - J_{xx}\right) - m_p l_{cg} r s_\theta \dot{\theta}^2 - b_1\dot{\psi} - b_{1c}\,\mathrm{sgn}\left(\dot{\psi}\right) \\ -m_p g l_{cg} s_\theta + s_\theta c_\theta \dot{\psi}^2\left(m_p l_{cg}^2 + J_{zz} - J_{xx}\right) - b_2\dot{\theta} - b_{2c}\,\mathrm{sgn}\left(\dot{\theta}\right) \end{Bmatrix}$$

Where the terms $b_{1c}\,\mathrm{sgn}\left(\dot{\psi}\right)$ and $b_{2c}\,\mathrm{sgn}\left(\dot{\theta}\right)$ are included to account for the presence of Coulomb friction in each revolute joint, g is the gravitational constant, and we are using the shorthand $\cos(\theta) = c_\theta$, and $\sin(\theta) = s_\theta$. J_{zz} and J_{xx} are the pendulum centroidal moments of inertia about axes perpendicular to its longitudinal axis, and due to symmetry, both equal the previously defined J_p. All other terms remain unchanged.

Students are then required to obtain experimental free-response data by lifting the pendulum to approximately horizontal, releasing, and observing the free response for large displacements. They then compare the experimental response to a numerical solution in order to refine estimates of poorly known system parameters. A simplex method is used to minimize the sum square difference between experimental response and numerical prediction. Typical agreement between the theoretical and experimental results after parameter optimization is shown in Figure 8.

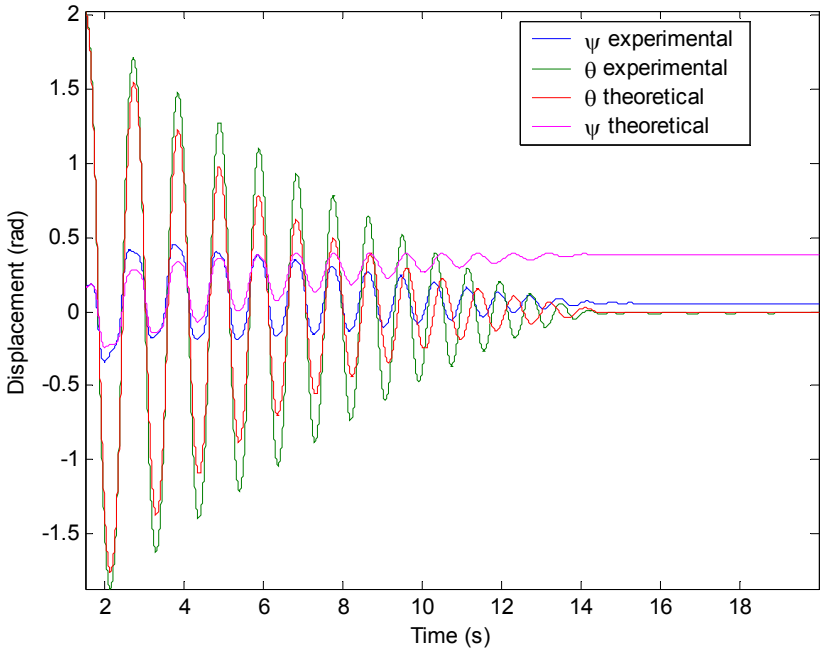

Fig 8. Typical Results from Advanced Dyanamics Experiment

As seen in Figure 8, agreement of the theoretical pendulum swing angle is satisfactory. The disk oscillation amplitude is captured well by the theoretical simulation, however, the selected initial conditions caused a definite drift due to the modeled rigid-body motion of the disk. This appears to be a numerical phenomenon. When observed in the experiment, such drift can be explained by imperfect alignment of gravity with the base disk axis, i.e. the apparatus not being level. In the case shown, the experimental shows no such drift. This observation leads to a suggested improvement for future use—that the disk should be anchored to the ground by a torsional stiffness. This will certainly reduce the amplitude of oscillations, but the stiffness can be

selected to be very soft, and the challenge of matching experimental and theoretical responses should be reduced significantly.

Assessment

Fifty-three (53) of the students enrolled in the introductory control class (ME 406) for the fall term of 2005 filled out a confidential self-assessment of their abilities prior to and after taking the course. The following three questions are regarded as relevant to this work since two of the four physical labs described above involve detailed modeling of mechanical systems.

Table 3. Student Self-Assessment Questions.

Question	Strongly Agree	Agree	Disagree	Strongly Disagree	I Don't Know
I understand the uses of models in designing control systems.	46%	54%	0%	0%	0%
I understand the limitations of models in designing control systems.	29%	65%	6%	0%	0%
This class has helped by better understand how modeling systems can be applied in engineering systems.	48%	45%	6%	0%	0%

The results are quite astounding. The first question has all respondents in the 'Strongly Agree' or Agree category. ME 406 emphasizes *model based* control design, so it is pleasantly surprising that students realize the importance of models. Also, in several cases, the students were unable to find a satisfactory model, and relied on parameters provided by the professor to complete their control system design. This perhaps served as further emphasis on the importance of having a good model.

The students were also asked to rate their knowledge of various course topics and self-confidence in being able to apply the knowledge gained. They provided self-assessment scores both prior to and after taking the course. The following scales were provided to guide the students' self-assessment:

Knowledge: What you know regarding this concept area.
4 = High, I know the concept and I have applied it in this course.
3 = Moderate, I know the concept but I still have not applied it.
2 = Low, I have only heard about the concept, but do not know it well enough to apply it.
1 = No Clue, I do not know the concept.

Confidence: Level of confidence you have in your ability to solve problems in this area.
4 = High, I am confident that I understand and can apply the concept to problems.
3 = Moderate, I am somewhat confident that I understand the concept and I can apply it to a new problem.
2 = Low, I have heard of the concept but I am not sure that I can apply it.
1 = No Clue, I am not confident that I can apply the concept.

The Pre and post course knowledge and confidence scores for the most relevant concept areas are shown in Table 4. In every category there is approximately 0.6 or better improvement. All improvements shown are statistically significant using a 95% confidence interval. The sample

size of 53 is certainly significant and represents by far the largest sample among the three courses surveyed.

It shouldn't surprise the reader that the area 'Benefits of Feedback control systems' and 'Size Limitations on control signals of real systems', saw the largest increases. As described above, these concepts were well emphasized in the lab by 1) the IP and FP experiments where an open-loop unstable plant was stabilized with feedback, and 2) both state feedback control experiments, where the closed-loop pole locations were intentionally chosen to push the actuator saturation limits.

Concluding Remarks

This paper has described four hardware based experiments for advanced mechanical system modeling and state feedback control. A post-course survey showed that the students' knowledge and confidence on the topics of model determination, benefits of feedback and limitations on the size of control signals were significantly increased.

Table 4. Student Self-Assessed Knowledge and Confidence.

Concept	Pre Course Knowledge	Pre Course Confidence	Post Course Knowledge	Post Course Confidence
Distinctions between a model and a real dynamical system	3.27	2.98	3.88	3.58
Various approaches to modeling dynamical systems	2.98	2.50	3.58	3.25
Comparisons between predicted response of a mathematical model and the response of a physical system.	3.15	2.79	3.75	3.42
Benefits of Feedback control systems	2.54	2.23	3.83	3.46
Size Limitations on control signals of real systems	1.60	1.50	3.02	2.69
Benefits of a state variable model	2.26	2.04	3.44	2.96

Acknowledgments

This material is based on work supported by the National Science Foundation under grant No. DUE-0310445. Any opinions, findings, and conclusions or recommendations expressed in this material are those of the author and do not necessarily reflect the views of the National Science Foundation. The author gratefully acknowledges the assistance of Shannon Sexton, Director of Assessment, who compiled the student responses, and did the statistical analysis showing significance of all differences.

References

1. Manual for Model 210/210a Rectilinear Control System, Educational Control Products, Bell Canyon, CA, 1999. http://www.ecpsystems.com
2. Xu, Y., Iwase, M., and Furuta, K., "Time Optimal Swing-Up Control of Single Pendulum," *Transactions of the ASME*, Volume 123, Sept 2001 Pages:518-527.
3. Burchett, B. T., "Parametric Time Domain System Identification of a Mass-Spring-Damper System", Proceedings of the 2005 American Society for Engineering Education Annual Conference & Exposition, Portland, OR, June 12-15, 2005.
4. Burchett, B. T., and Layton, R. A., "An Undergraduate System Identification Laboratory", Proceedings of the 2005 American Control Conference, Portland, OR, June 8-10, 2005.

Author Biography

BRADLEY T BURCHETT is an Assistant Professor of Mechanical Engineering. He teaches courses on the topics of dynamics, system dynamics, control, intelligent control, and computer applications. His research interests include non-linear and intelligent control of autonomous vehicles, and numerical methods applied to optimal control.

Appendix

Here we show the equations of motion for the linear pendulum system in crane and inverted mode. The system parameters and coordinates are defined in Figure A1.

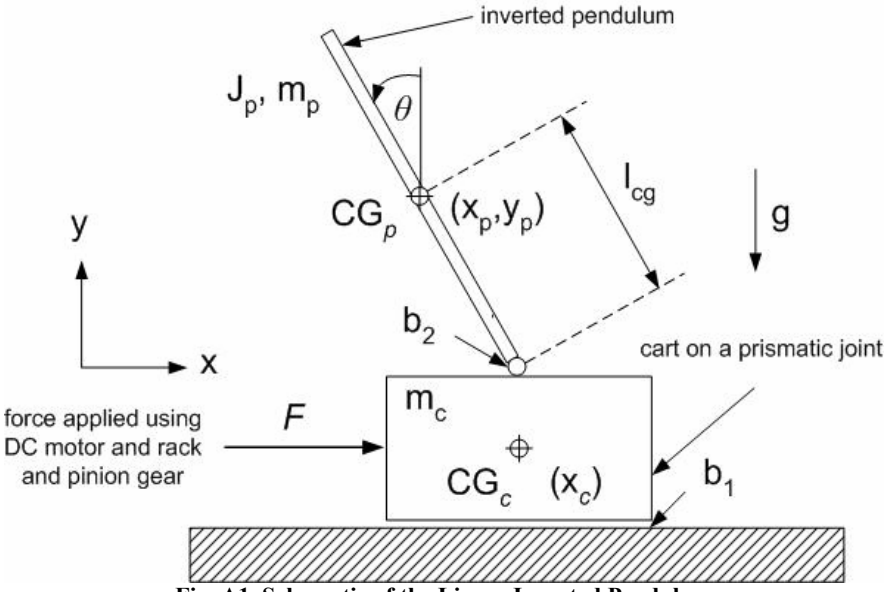

Fig. A1. Schematic of the Linear Inverted Pendulum

The linearized state space model in crane mode is.

$$\dot{\mathbf{x}} = \mathbf{A}\mathbf{x} + \mathbf{B}F \qquad (1)$$
$$\mathbf{y} = \mathbf{C}\mathbf{x}$$

Where

$$\mathbf{A} = \begin{bmatrix} 0 & 1 & 0 & 0 \\ 0 & \dfrac{-J_A b_1}{D} & \dfrac{m_p^2 l_{cg}^2 g}{D} & \dfrac{m_p l_{cg} b_2}{D} \\ 0 & 0 & 0 & 1 \\ 0 & \dfrac{m_p l_{cg} b_1}{D} & -\dfrac{\left(m_c + m_p\right) m_p l_{cg} g}{D} & -\dfrac{\left(m_c + m_p\right) b_2}{D} \end{bmatrix}$$

$$\mathbf{B} = \begin{bmatrix} 0 & \dfrac{J_A}{D} & 0 & -\dfrac{m_p l_{cg}}{D} \end{bmatrix}^T$$

$$\mathbf{C} = \begin{bmatrix} K_1 & 0 & 0 & 0 \\ 0 & 0 & K_2 & 0 \end{bmatrix}$$

$$\mathbf{x} = \begin{bmatrix} x & \dot{x} & \theta & \dot{\theta} \end{bmatrix}^T$$

$$D = J_A\left(m_c + m_p\right) - m_p^2 l_{cg}^2$$

and

$$J_A = J_p + m_p l_{cg}^2.$$

The corresponding state matrices for inverted mode are:

$$\mathbf{A} = \begin{bmatrix} 0 & 1 & 0 & 0 \\ 0 & \dfrac{-J_A b_1}{D} & \dfrac{m_p^2 l_{cg}^2 g}{D} & -\dfrac{m_p l_{cg} b_2}{D} \\ 0 & 0 & 0 & 1 \\ 0 & -\dfrac{m_p l_{cg} b_1}{D} & \dfrac{\left(m_c + m_p\right) m_p l_{cg} g}{D} & -\dfrac{\left(m_c + m_p\right) b_2}{D} \end{bmatrix}$$

$$\mathbf{B} = \begin{bmatrix} 0 & \dfrac{J_A}{D} & 0 & \dfrac{m_p l_{cg}}{D} \end{bmatrix}^{\mathrm{T}}$$

The state definition, output matrix (**C**), and intermediate quantities remain unchanged.